Journal of Sound and Vibration (1998) **218**(3), 463–479
Article No. sv981815

IMPROVED METHODS FOR ESTIMATING FITTING DENSITY IN INDUSTRIAL WORKROOMS

K. Li and M. Hodgson

Occupational Hygiene Programme and Department of Mechanical Engineering, University of British Columbia, 3rd Floor, 2206 East Mall, Vancouver, BC, Canada V6T 1Z3

(*Received* 16 *January* 1998, *and in final form* 22 *June* 1998)

When predicting sound fields in rooms such as industrial workrooms, a major factor that must be taken into consideration is the presence of 'fittings'—obstacles such as machines, work-benches and stockpiles—in the room. Besides the fitting spatial distribution, there are two important parameters used in prediction models to describe the fittings. One is the fitting density—a measure of the number of fittings and of the average fitting scattering cross-sectional area; the other is the fitting absorption coefficient. While ranges of typical fitting densities and absorption coefficients are known, no reliable method exists for measuring or estimating them in a given case. Furthermore, theoretical expressions for calculating fitting density assume small fittings and high frequency. The aim of this research was to develop and test new, improved methods for determining the fitting density in industrial workrooms. To achieve this objective a correction formula was derived for calculating the fitting density in the case of large fitting dimension. The variation of fitting density with frequency was found from sound-propagation measurements in large fitted regions. A formula to express the relationship was determined by statistical methods. This model was validated experimentally in a scale-model workroom and in a machine shop, with the help of a ray-tracing prediction model.

1. INTRODUCTION

Industrial workrooms are different from many other rooms in that they are not empty—they are "fitted"; that is, they contain many obstacles (machines, stockpiles, benches etc.—the "fittings") which scatter and absorb propagating sound. Fittings have a major effect on the magnitude and spatial distribution of noise levels in an industrial workroom, as well as on the rate of sound decay with time and, thus, on reverberation time [1].

Analytical models for predicting sound-pressure levels in industrial workrooms exist which account for the presence of fittings. The Jovicic [2] and Lindqvist [3, 4] models are based on the image-source method; to calculate the total sound energy, the received unscattered and scattered energies are treated separately and then summed. The Jovicic model [2] can be applied to long, or long and wide,

0022–460X/98/480463 + 17 $30.00/0

parallelepipedic rooms with isotropically distributed fittings. The Lindqvist model [3, 4] can be applied to any parallelepipedic room with isotropically distributed fittings. The Ondet and Barbry model [5] is based on ray-tracing techniques. Fittings, with representative fitting densities and absorption coefficients, are randomly distributed within any number of predefined zones. This is the only model which is able to account for arbitary distributions of fittings, and non-parallelepipedic rooms with diverse absorption characteristics. Dance and Shield [6] used a method-of-images approach to develop a model applicable to parallelpipedic workrooms. Fitted rooms contained horizontal and/or vertical fitted zones, in which fittings resulted in an exponential reduction with distance of propagating sound energy.

There are three main factors which must be considered in fitted rooms, as compared to empty rooms: the fitting spatial distribution (isotropic, localized to a layer on the floor, etc.); the absorption coefficient of the fittings; the "fitting density". The last two quantities would be expected to vary with frequency. While the orders of magnitude of these two quantities are known [7], no reliable, generally-applicable method is available for determining these quantities directly. Furthermore, theoretical expressions for calculating fitting density assume small fittings and high frequency.

"Fitting density" describes the average frequency at which propagating sound rays encounter fittings. Fitting density Q—defined as the product of the number of fittings per unit volume and their average scattering cross-sectional area, in m^{-1}, is a very important parameter in predicting sound-pressure levels in fitted workrooms [1]. Almost all existing prediction models use the Kuttruff fitting-density formula [8] to calculate this parameter. The Kuttruff formula can be written as $Q_0 = S_{tot}/4V$, in which Q_0 is the Kuttruff fitting density in m^{-1}, V is the total room volume in m^3, and S_{tot} is the total surface area of the fittings in m^2. The Kuttruff formula is valid for high frequencies and for small fittings, but is used by practitioners for all frequencies and fitting dimensions.

In summary, there is a great need for accurate, proven methods for calculating fitting density and fitting absorption coefficient—and their variations with frequency—in the case of large fittings. The main objective of the present research was to develop and test improved methods for determining fitting density in industrial workrooms. Methods have been developed based on measurements of steady state sound-pressure level in empty and fitted environments. The methods have been validated in an anechoic chamber, in a 1:8-scale-model workroom and in a full-scale machine shop.

2. EXISTING MODELS OF SOUND PROPAGATION IN FITTED REGIONS

Let us review existing theory for sound propagation in fitted regions. When a sound ray is emitted from a source in a fitted region, its propagation is affected by the presence of the obstacles, as shown in Figure 1. When there are large numbers of obstacles with different shapes and orientations, it becomes impractical to describe the influence of each of them separately. Therefore, a statistical

approach to the problem becomes preferable. This high-frequency approach, proposed by Kuttruff [8], is based on the following hypotheses.

1. High-frequency sound waves propagate as rays (the geometrical-acoustics assumption).
2. The obstacles are point-like scattering objects reradiating sound rays omni-directionally. The validity of this hypothesis would be expected to depend on the ratio of the wavelength λ of the sound wave to the typical dimension D_f of the obstacle. As a general rule, one must have $\lambda < D_f$—that is, small obstacles.
3. The scattering effect follows a Poisson process. This means that, if the energy emitted by the source is discretized into sound particles, and if the fact of one of these particles meeting an obstacle is a random event, then the sequence of random events follows a Poisson distribution. However, it must be supposed that the number of obstacles encountered by a particle between times t and $t + \mathrm{d}t$ is independent of the number of obstacles encountered before time t. Under this assumption, the probability W_k that a sound particle hits k obstacles after times t_k. can be expressed as

$$W_k(ct_k) = \exp(-Qct_k)(Qct_k)^k/k!. \tag{1}$$

The cumulative distribution function $F(r)$ associated with this distribution is

$$F(r) = \begin{cases} 1 - \exp(-Qr), & r \geqslant 0, \\ 0, & r < 0. \end{cases} \tag{2}$$

The number of fittings per unit volume can be expressed by $n = N_f/V$, where N_f designates the number of obstacles contained in volume V. Let S_f by the average scattering cross-sectional area of an obstacle. This is difficult to determine accurately when the obstacles have complex shapes. The simplest solution is to approximate the shape by a sphere with diameter d and surface area $S_v = \pi d^2$. The average scattering cross-sectional area, for high frequency, is then equal to the visible cross-sectional area of the equivalent sphere, given by $S_f = \pi d^2/4$. Therefore, $S_f = S_v/4$. Consequently, in volume V, the average cross-sectional area per unit

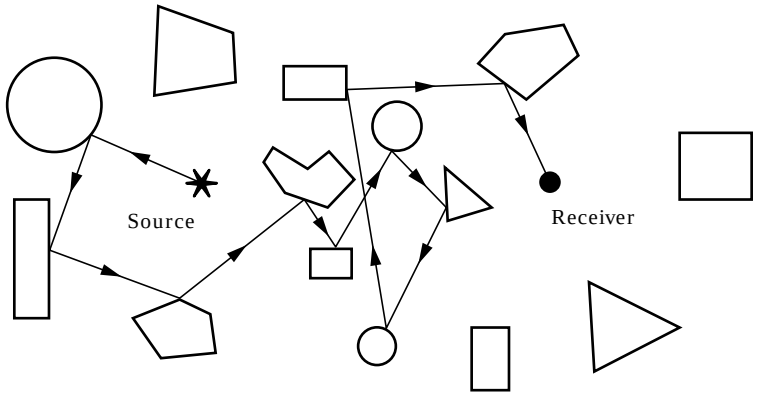

Figure 1. A single sound-ray propagation path in a fitted region.

volume, called the Kuttruff fitting density—also known as the scattering frequency [2–5]—is given by the expression

$$Q_0 = nS_f = nS_v/4 = S_{tot}/4V. \tag{3}$$

Again, this formula is valid for very high frequency and for obstacles which are small and spherically shaped, but it is used in most prediction methods and by practitioners with little regard to its applicability. Note that the quantity $l_f = 1/Q_0$ in metres is the mean free-path length between fittings.

Lindqvist [3] gave a formula for correcting for the possibility of overlap of fittings in the Poisson process, based on a two-dimensional analysis. Lindqvist supposed that there is a Poisson distribution of fittings with density Q, and considered two identical spheres of radius R, which overlap. The probability density of no second fitting being found within a distance r of the centre of a fitting is $f(r) = Q\mathrm{e}^{-Qr}$. The probability function for no fitting within a distance $2R$ is, thus,

$$F(2R) = \int Q\mathrm{e}^{-Qr}\mathrm{d}r = 1 - \mathrm{e}^{-2QR}. \tag{4}$$

From this, Lindqvist [3] found the following approximate correction formula

$$Q_L = Q_0[1 + (8Q_0R/3\pi) - Q_0^2R^2/2], \tag{5}$$

in which Q_0 is the Kuttruff fitting density. For example, if $Q_0R = 0{\cdot}1$, the correction increases the fitting cross-sectional area, and therefore the fitting density, by 8%. Kurze [9] noted that, in many cases, the fitting density found using equation (3) is smaller than expected, so higher surface-absorption coefficients must be used in prediction to obtain agreement with temporal sound-decay measurements. Kurze suggested the use of somewhat different statistical relations. The shifted distribution is one possible candidate: in the range $r_0 \leqslant r < \infty$, the mean free-path l_f becomes $l_f = 1/Q_0 - r_0$ where r_0 is some distance. This means that the fitting mean free-path is smaller than that calculated from equation (3) by an amount equal to the distance r_0. In the case of numerous fittings of different dimensions, r_0 can be considered to be the average radius of the fittings. Another possibility for arriving at a reduced mean free-path length is to use the Gamma distribution. In this case, the mean free-path becomes $l_f = 1/Q_0p$ in which p is the parameter in the Gamma function $\Gamma(p)$. For $p = 1$ this equation is a special case of equation (3); for $p > 1$, l_f is less than $1/Q_0$, so better consistency between absorption coefficients and measured rates of reverberant sound decay is obtained [9].

Hodgson [10] measured noise levels in a machine shop and compared them with ray-tracing predictions using different fitting-density values. A best-fit fitting density was obtained which was about 40% greater than that calculated using the Kuttruff formula.

Akil and Oldham [11, 12] concluded that it is the product of fitting density and fitting absorption coefficient that determines the sound-propagation characteristics in a fitted workroom. They found that the difference in sound-pressure level in a room with fittings and without fittings is almost constant, and that the

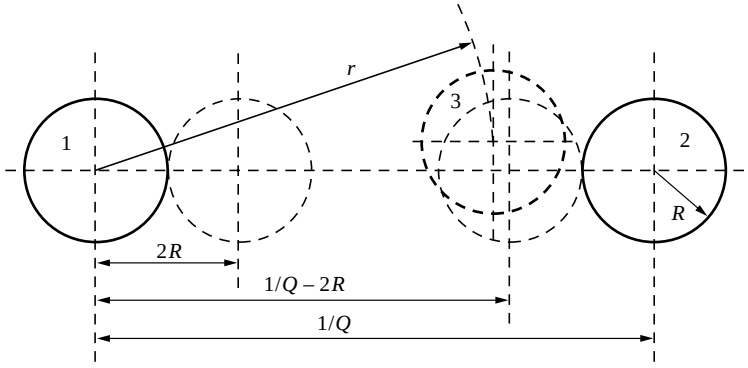

Figure 2. Three spheres of radius R considered in estimating the mean free-path reduction.

sound-propagation characteristics are nearly identical if one parameter is halved and the other is doubled.

Hodgson [7] used a best-fit approach to determine fitting densities in typical industrial workrooms with relatively low and high fitting absorption coefficients (0·5 and 0·15, respectively) and two vertical fitting distributions (isotropic and in a layer on the floor). With an isotropic vertical fitting distribution, fitting densities varied from 0·07 to 0·25 m^{-1} with the lower coefficient, and from 0·04 to 0·125 m^{-1} with the higher one. With a fitting floor layer, fitting densities varied from 0·40 to 1·10 m^{-1} and 0·15 to 0·30 m^{-1} with the lower and higher coefficients, respectively.

In summary, methods exist for estimating fitting density, but all assume small dimension and high frequency. Some empirical information is available on typical fitting densities.

3. THEORETICAL DEVELOPMENT

In this section, a correction formula for calculating fitting density in cases when the fitting dimensions are large is derived, and the magnitude of the correction is investigated.

When the mean free-path, $l_{f0} = 1/Q_0$, is of the same order of magnitude as, or one order greater than, the fitting dimension, the fitting dimension should be subtracted from the mean free-path, as shown in Figure 2. That is,

$$1/Q = 1/Q_0 - 2R. \tag{6}$$

Considering the dimensions of typical fittings, a further correction should be included. In Figure 2, there is a third fitting (3) near the other two (1 and 2). If the third fitting is dimensionless, it will not block the sound propagating from fitting 1 to fitting 2. However, if the fitting has non-zero dimension, it does block this path. The real propagation path will be from fitting 1 to fitting 3; it is less than from fitting 1 to fitting 2, the mean free-path l_{f0}.

Suppose that there is a Poisson distribution of fittings with density Q_0, and consider three identical spheres of radius R, as shown in Figure 2. From equation (4), the probability function for no fitting within distance r is $\exp(-Q_0 r)$. This

is only true for dimensionless fittings. The probability function for having a fitting within distance r is $1 - \exp(-Q_0 r)$, and the probability that the fitting blocks the free path is $2R/2\pi r$, considering the fitting dimensions shown in Figure 2. For a two-dimensional problem, for any position from the centre of a fitting in a region of a circle from 0 to 2π, and distance r from $2R$ to $1/Q_0 - 2R$, the probability for the fitting with radius R blocking the original mean free-path is $2R[1 - \exp(-Q_0 r)]/(2\pi r)$. For the region $0 < r < 2R$ and $1/Q_0 - 2R < r < 1/Q_0$, it will be possible for the fittings to overlap, as corrected by the Lindqvist formula, equation (5). The further reduction of mean free-path can be written as

$$\Delta(1/Q) = \int_{0^-}^{2\pi^+} \int_{2R}^{1/Q_0 - 2R} [1 - \exp(-Q_0 r)](2R/2\pi r)\, \mathrm{d}\Theta\, \mathrm{d}r. \tag{7}$$

Replacing $\exp(-Qr)$ by $(1 - Qr)$, an approximate expression is obtained:

$$\Delta(1/Q) = 2R - 8R^2 Q_0. \tag{8}$$

From equations (6) and (8), the total reduction of mean free-path is

$$\Delta l_f = 4R - 8R^2 Q_0. \tag{9}$$

Replacing $2R$ by the mean fitting dimension D_f, the corrected fitting density becomes

$$Q'' = [(1/Q_0) - 2D_f + 2Q_0 D_f^2]^{-1}. \tag{10}$$

Combining the new correction with that of Lindqvist, equation (5), the fitting density can be written as

$$Q' = [1/aQ_0) - 2D_f + 2Q_0 D_f^2]^{-1}, \tag{11}$$

in which a is the correction factor given by Lindqvist,

$$a = 1 + (8Q_0 D_f/3\pi) - (Q_0^2 D_f^2/2), \tag{12}$$

and Q_0 is calculated by the Kuttruff formula, equation (3). The effect of the new correction depends on D_f and Q_0. For example, if $Q_0 = 0{\cdot}1\ \mathrm{m}^{-1}$ and $D_f = 1$ m, the fitting mean free-path will decrease from 10 m to 8·2 m, and the fitting density will increase to $0{\cdot}122\ \mathrm{m}^{-1}$, which is 22% larger than Q_0. As is the case for equation (3), equation (11) is only valid for high frequency.

TABLE 1

Fitting densities (in m^{-1}) calculated by various methods (see text)

	$D_f = 0{\cdot}5$ m			$D_f = 1$ m			$D_f = 2$ m			$D_f = 5$ m		
Q_0	Q_L	Q''	Q'	Q_L	Q''	Q'	Q_L	Q''	Q'	Q_L	Q''	Q'
0·05	0·051	0·053	0·054	0·051	0·055	0·056	0·052	0·061	0·064	0·055	0·080	0·094
0·10	0·102	0·110	0·113	0·104	0·122	0·128	0·108	0·147	0·165	0·118	0·200	0·288
0·15	0·155	0·174	0·181	0·159	0·201	0·218	0·167	0·259	0·314	0·187	0·240	0·351

Table 1 shows some typical fitting densities corrected by equations (5) and (11). The first column gives the Kuttruff Q_0. The other columns show the corrected values for $D_f = 0{\cdot}5$, 1, 2, and 5 m, respectively. In each case, the left value is Q_L from the Lindqvist formula, equation (5), the middle value is Q'' from equation (10) and the right value is Q' from equation (11). We can see that the differences in fitting density are small for small Q_0 and D_f, but that they are large when D_f and Q_0 are large. For the extreme case of $Q_0 = 0{\cdot}15\ \mathrm{m}^{-1}$ and $D_f = 5$ m, Q' is 134% greater than Q_0. This can be explained by considering a hypothetical region fitted with N_f spherical fittings of diameter 5 m. The dimensions of the region are $100 \times 100 \times 100\ \mathrm{m}^3$. The surface area of a sphere is $S_v = \pi D_f^2 = 78{\cdot}54\ \mathrm{m}^2$; from the Kuttruff formula, $N_f = 4VQ_0/S_v = 7639{\cdot}4$. If the spheres are uniformly distributed in three dimensions, the distance between the centers of the two spheres is $100/7639{\cdot}4^{1/3} = 5{\cdot}08$ m. This is just slightly larger than the sphere diameter; the mean free-path between the fittings is much smaller than $1/Q_0 = 1/0{\cdot}15 = 6{\cdot}67$ m, so $1/Q' = 1/0{\cdot}351 = 2{\cdot}85$ m, calculated using equation (11), seems reasonable. This analysis assumes a uniform distribution of fittings; it is clear that the spheres could not in fact be distributed randomly in this region.

4. EXPERIMENTAL METHODS

This section discusses the experimental methodology used in the validation of the new theoretical models, and the instrumentation involved. Tests were performed in an anechoic chamber and in a test enclosure—both considered as 1:8-scale models—using the Maximum Length Sequence System Analyzer (MLSSA). The principles of scale modelling, as applied to industrial workrooms, are discussed in detail elsewhere [13]. In a 1:8-scale model, sound frequencies are scaled up 8 times. The dimensions of all fittings are scaled by 1/8, in which case wavelength-to-dimension ratios are preserved, and fitting density scales up by 8. A scale factor of 8 was chosen because the mean dimension of the objects used as scale-model fittings corresponded to the mean dimensions of typical large, full-scale fittings in industrial workrooms. Also, the anechoic chamber corresponded to a sufficiently large, unbounded region at 1:8 scale. Furthermore, a scale factor of 8 has the advantage that model-scale octave-band frequencies, when scaled to full-size eqivalents, correspond to standard octave-bands. In most industrial applications, the 125–4000 Hz octave bands are most important. These correspond to a 1:8-scale-model frequency range of 1000–32000 Hz—the range involved in all model tests. No attempt was made to accurately scale air absorption which was, therefore, excessive in the scale model. However, this does not affect results based on comparisons of prediction with experiment, as in this paper, as long as predictions are done using air-absorption values applicable to the air absorption present in the experiments.

4.1. MEASUREMENT SYSTEM

Measurements were made in different test environments using the same measurement system. The MLSSA system generated test signals which were amplified by an MB100 power amplifier and radiated by the scale-model sound

source. Sound waves propagating in the test environment were received by a Bruel & Kjaer 4135 microphone; the resulting signals were amplified by a Bruel & Kjaer 2609 measuring amplifier and analyzed by MLSSA system.

The model sound source consisted of a 75-mm diameter, Realistic 40-1289A mid-range tweeter loudspeaker with a reversed fibre-glass cone narrowing to a 3-mm diameter opening attached to it to make the source omni-directional over the test frequency range. The sound power of the loudspeaker was calculated from sound-pressure levels measured in a free-field environment.

4.2. SCALE-MODEL FITTINGS

In order to model sound propagation in fitted regions, empty 18·9-l mineral-water bottles were used as fittings. These hard-plastic bottles were 40 cm high and 27·5 cm in diameter (3·2 by 2·2 mFS—FS means full-scale equivalent value). The bottles were capped to prevent their acting as Helmholtz resonators. The reason for choosing these bottles was that their size was suitable for 1:8 scale modelling of industrial fittings of large dimension, and because the absorption coefficient of the bottle surface was low. The surface area, S_v, of one bottle was approximately 0·46 m^2 (29·4 mFS^2); the mean dimension was 0·3 m (2·4 mFS).

4.3. TEST ENVIRONMENTS

4.3.1. *Anechoic chamber*

A fully anechoic chamber was used as a test environment to approximate an infinite region. Its dimensions were $4{\cdot}7 \times 4{\cdot}1 \times 2{\cdot}4$ m high ($37{\cdot}6 \times 32{\cdot}8 \times 19{\cdot}2$ mFS high when considered as a 1:8-scale model). Sound-propagation tests were performed in the empty anechoic chamber to confirm that it was an excellent approximation to a free field at the model test frequencies, as long as the source and receiver were not close to the chamber walls. Similarly, the anechoic chamber, fitted with water bottles, was used to study sound propagation in an approximately infinite fitted region. In order to validate its use, ray tracing was used to compare the sound field in the fitted chamber with that in an approximately infinite fitted region. An infinite region was approximated as a room with dimensions of $100 \times 100 \times 100$ m. The source was located at the middle of both regions. The differences in sound-pressure levels in the two regions were less than 1 dB if the source was at the middle of the chamber, and if the source/receiver distance was less than half the distance to the chamber surfaces. However, the differences were large when the source or the receiver was near any room surface; the differences increased with fitting density, and with the source/receiver distance, by up to 3 dB at $r = 2$ m with $Q = 0{\cdot}5\ m^{-1}$. To avoid problems associated with the finite size of the chamber, the source/receiver distance was limited to 1·25 m and the source was always located in the middle of the chamber. Used in this way, the anechoic chamber was an adequate approximation to an infinite region.

Tests were performed in the anechoic chamber when empty, and when fitted with three fitting densities involving 81, 162 or 243 bottles. Given the anechoic-chamber volume of 46·2 m^3, and using the Kuttruff formula of equation

Figure 3. The fitted, 5-mFS-high, 1:8-scale model with absorbent ceiling. The front doors are open and the left roof tilted up to reveal the inside.

(3), these corresponded to fitting densities of $0{\cdot}2\,\mathrm{m}^{-1}$ ($0{\cdot}025\,\mathrm{mFS}^{-1}$), $0{\cdot}4\,\mathrm{m}^{-1}$ ($0{\cdot}05\,\mathrm{mFS}^{-1}$), and $0{\cdot}6^{-1}$ ($0{\cdot}075\,\mathrm{mFS}^{-1}$), respectively. These full-scale fitting densities are typical of low-density and moderately-densely-fitted workrooms [7]. It was not feasible to test higher densities.

4.3.2. *Scale-model workroom*

Tests were also done in a more realistic environment—a 1:8-scale-model industrial workroom. Figure 3 is a photograph of the model. It was 3·75m (30 mFS) long, 1·875 m (15 mFS) wide, and either 1·875 m (15 mFS) or 0·625 m (5 mFS) high. The vertical walls and the ceiling were made of varnished plywood, and the floor was of concrete. The average absorption coefficients of the surfaces were determined by comparing sound-progation curves measured in the empty model with those predicted by ray tracing for various coefficient values until the best-fit coefficient was found.

5. EMPIRICAL DETERMINATION OF FREQUENCY-VARYING FITTING DENSITY

5.1. INTRODUCTION

This section presents details of experiments performed in the anechoic chamber to determine the fitting density in fitted regions and to derive a relationship for the variation of fitting density with frequency. As discussed in section 4.3, the chamber was fitted with 81, 162 or 243 bottles; these were arranged randomly in the chamber in three dimensions. It was found that when the number of bottles

was large, it was impossible to arrange the bottles completely randomly, since sometimes bottles were too close. Octave-band sound-pressure levels were measured at 8–20 positions at each source/receiver distance, and average levels calculated.

5.2. SOUND-ENERGY CONTRIBUTIONS

Regarding sound propagation in fitted regions, we can differentiate between sound-pressure levels measured at a receiver location in two cases—when the direct sound is not blocked, and when it is blocked by fittings. The total sound energy is the sum of two parts—the scattered part and the unscattered part. The unscattered sound-energy density E_u was derived by Kuttruff [8] as

$$E_u = W \exp(-rQ)/4\pi r^2 c = E_{Q=0} \exp(-rQ), \tag{13}$$

in which $E_{Q=0} = W/4\pi r^2 c$; W is the source sound power, and c is the sound speed in air. The sound energy can be related to the sound-pressure level L_p, using $E = 10^{L_p/10}/c$. Thus, equation (13) can be rewritten as

$$E_u = 10^{L_{p,u}/10}/c = (10^{L_{p,Q=0}/10}/c) \exp(-rQ). \tag{14}$$

Following are the definitions of some relevant sound energies. $E_{Q=0}$: the sound energy measured in a free field with $Q = 0\ \mathrm{m}^{-1}$—that is, when there is direct sound and no scattered sound. E_t: the total sound energy. In a fitted room this is the sum of the unscattered and scattered energies. E_u: the unscattered part of total sound energy. E_s: the scattered part of the total sound energy. E_b: the sound energy for the case when there are one or more fittings blocking the direct sound. E_b is not the same as E_s, because the fittings are not dimensionless. They block not only the direct sound, but also some scattered sound; thus, E_b is generally less than E_s. E_{nb}: the sound energy for the case when there is no fitting blocking the direct sound.

The following relationships between these sound-energy components exist: $E_t = E_u + E_s$; $E_s = E_{nb} - E_{Q=0}$. Thus, the unscattered sound energy can be expressed as $E_u = E_t - E_s = E_{Q=0} - E_{nb} + E_t$. Since $E_u = E_{Q=0} \exp(-rQ)$, dividing both sides of by $E_{Q=0}$ results in $\exp(-rQ) = 1 - (E_{nb} - E_t)/E_{Q=0}$. Thus, the fitting density Q is dependent on three measurable quantities which all vary with frequency. The variation of Q with frequency is given by

$$Q(f) = -(1/r) \ln \{1 - [(E_{nb}(f) - E_t(f)]/E_{Q=0}(f)\}. \tag{15}$$

Figure 4 shows the values of $Q(f)$ derived, using equation (15), from the measurements in the fitted anechoic chamber with the three densities of fittings. Table 2 gives the corresponding fitting densities calculated using the Kuttruff formula (Q_0, equation (3)), from the Lindqvist corrected formula (Q_L, equation (5)), and by the new formula (Q', equation (11)). These values are also shown in Figure 4. The fitting density varies significantly with frequency. Measured fitting densities are much higher than the Kuttruff fitting density Q_0 at high frequencies, much lower at low frequencies, but equal to the Kuttruff values at some intermediate frequencies. The Lindqvist correction formula gives approximately the same results as the Kuttruff formula, since the correction involved in Q_L

increases the fitting-density values by less than 8% in these cases. The values obtained by the new correction formula agree well with those measured at high frequencies, as expected.

5.3. AN EMPIRICAL MODEL FOR $Q(f)$

According to Figure 4, a non-linear model must be used to express the relationship between fitting density and frequency. After considering several models, the following model was chosen:

$$Q(f) = Q_\infty/(1 + Af_0/f), \tag{16}$$

in which $Q_\infty = Q(\infty)$, f is frequency, f_0 is a hypothetical fundamental frequency which depends on the mean fitting dimension D_f, with $f_0 = c/D_f$, and c is sound speed in air. In our experiments with water bottles, $D_f = 0{\cdot}3$ m and $c = 344$ m/s, so $f_0 = 1136$ Hz. An estimate for A in equation (16) can be found from experimental data using regression techniques. The resulting best-fit variation of Q with frequency can be approximated by

$$Q(f) = Q_\infty/(1 + 1{\cdot}2f_0/f). \tag{17}$$

In Figure 5, the measured data for $Q(f)/A_\infty$ are compared with the prediction by equation (17). We can see that equation (17) is a reasonable model of the variation of average fitting density with frequency.

Note that, with the hypothetical fundamental frequency included, since f_0 depends on the fitting dimension, this model in principle allows that parameter to be taken into consideration. Unfortunately, it was not feasible to perform experiments with more than one fitting dimension to verify the relationship.

6. EXPERIMENTAL VALIDATION

Comparisons were made between predictions and measurements of sound propagation (*SP*—the received sound-pressure level minus the source sound-power level, in decibels) in a 1:8-scale-model industrial workroom and in a full-size machine shop. The objective was to validate the correction formula for fitting density, equation (11), and the model of frequency-varying fitting density, equation (17).

TABLE 2

Fitting densities (in m^{-1}) relevant to the tests in the fitted anechoic chamber calculated by three methods (see text). n is the number of bottles

n	Q_0	Q_L	Q'
81	0·2	0·205	0·232
162	0·4	0·420	0·541
243	0·6	0·643	0·944

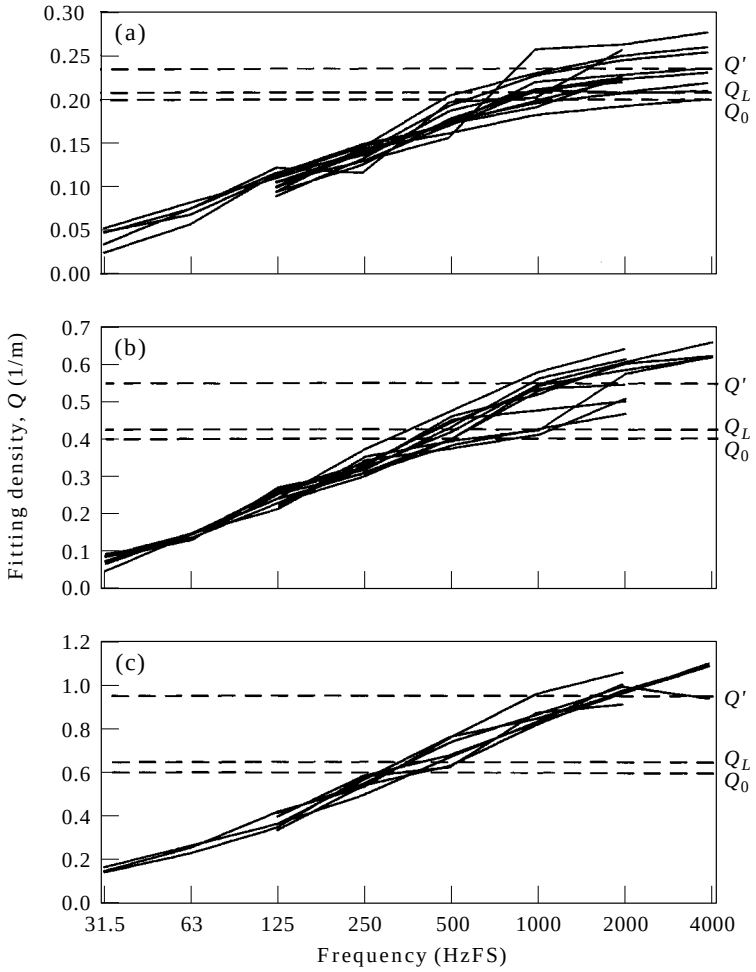

Figure 4. Variation of fitting density Q with frequency as calculated from experimental data using equation (15): (a) $Q_0 = 0{\cdot}2$ mFS^{-1}; (b) $Q_0 = 0{\cdot}4$ mFS^{-1}; (c) $Q_0 = 0{\cdot}6$ mFS^{-1}. Also shown in each case are the fitting densities Q_0, Q_L and Q'.

6.1. SCALE-MODEL WORKROOM

Experiments were done in the 1:8-scale model, configured as a typical industrial workroom with an acoustically treated (covered with 50-mmFS-thick glass fibre) ceiling at a height of 5 mFS. The source was 1·0 mFS high, at half width, and at 2·5 mFS from one end wall. Receiver positions were 1·5 mFS high, at half width, and at source/receiver distances of 1, 2, 5, 10, 15, 20 and 25 mFS. The fittings consisted of 31 bottles placed upside-down in a uniform distribution on the floor—as shown in Figure 3—with a 1-mFS-high void above. The fitting density calculated by the Kuttruff was 0·1 mFS^{-1}; the corrected value calculated by equation (11) was 0·183 mFS^{-1}.

First the empty room was measured and predicted, to determine the effective ceiling-absorption coefficients using the best-fit method; the results, along with the other input parameter values, are shown in Table 3.

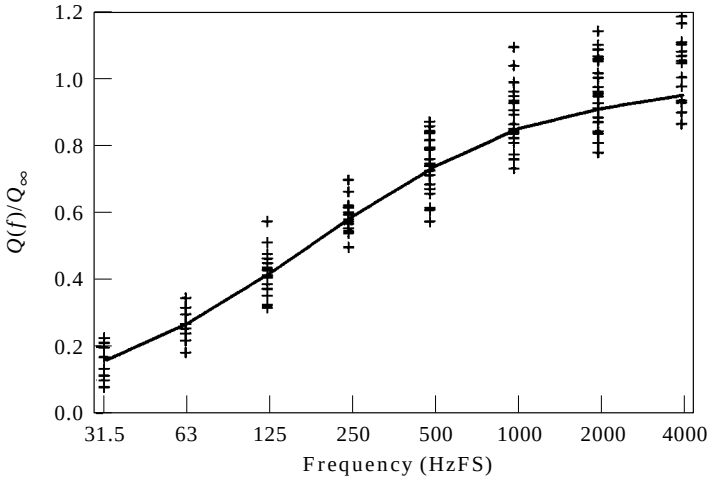

Figure 5. Variation of Q/Q_∞ with frequency: +, as determined from experimental data using equation (15); ——, as predicted by equation (17).

Figure 6 compares the measured results at 4000 Hz with those predicted by ray tracing using Q_0 and $Q(f)$. The differences between the sound-propagation values predicted using Q_0 and $Q(f)$ increase with source/receiver distance to about 3·5 dB. Results are similar at lower frequencies, though the magnitudes of the differences increase with frequency, as expected. The sound-propagation curves predicted using $Q(f)$ are in excellent agreement with the measured curves at all distances and frequencies. The validity of the new correction formula, equation (11), and the model for $Q(f)$, equation (17), are supported by these experimental results.

6.2. MACHINE SHOP

Comparisons were made with data from Hodgson's work [10], which involved ray-tracing prediction of sound-propagation curves in a fitted machine shop. The dimensions of the shop were 46 × 15 × 7·2 m high. The floor of the room was of concrete, its walls were made of unpainted blockwork, and its ceiling was of typical

TABLE 3

The parameters used in prediction for the scale-model workroom with uniformly distributed fittings on the floor. m is the air-absorption exponent

Parameter	Octave band (Hz)				
	250	500	1000	2000	4000
m (Np/m)	0·00035	0·00073	0·0021	0·0075	0·025
α (ceiling)	0·40	0·45	0·40	0·40	0·30
α (other surfaces)	0·05	0·05	0·05	0·05	0·05
α (fittings)	0·01	0·02	0·02	0·03	0·04
Q_0 (mFS^{-1})	0·1	0·1	0·1	0·1	0·1
$Q(f)$ (mFS^{-1})	0·109	0·137	0·157	0·169	0·176

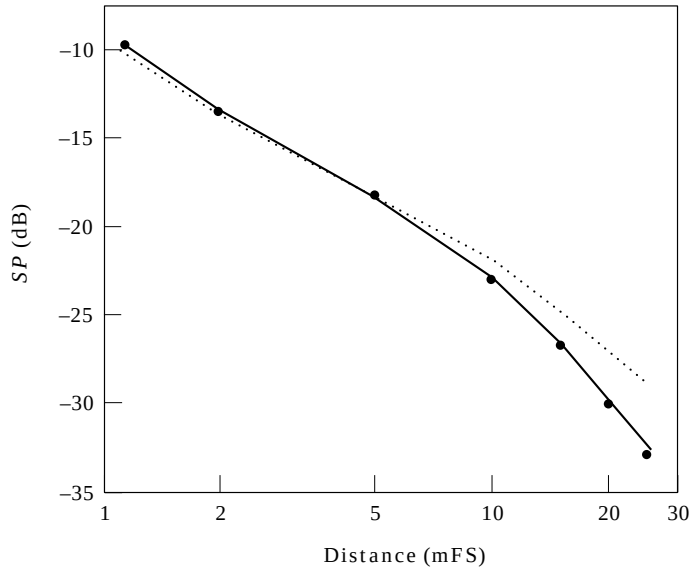

Figure 6. 4000-HzFS octave-band sound-propagation curves for the fitted 1:8-scale model: ●, measured; predicted by ray tracing with fitting densities Q_0 (· · · · ·) and $Q(f)$ (——).

steel-deck construction (consisting of corrugated metal inside, insulation, and a vapour barrier and gravel outside). The roof was supported by metal trusswork. The average octave-band absorption coefficients of the surfaces were estimated from measurements of reverberation time in nominally-empty buildings of the same construction, and have been found to vary little from one building to another [14]. The resulting coefficients were 0·12 at 250 Hz, 0·1 at 500 Hz, 0·08 at 1000 Hz, and 0·06 at 2000 and 4000 Hz.

The machine shop contained a total of 63 major fittings, distributed fairly uniformly over the floor area. The fittings included machine tools and other equipment, work benches, cabinets, and stock piles, with an average fitting height of about 1·5 m. The total fitting surface area, as calculated from the dimensions of rectangular boxes that would just enclose the fittings, was 675·5 m^2; thus, $Q_0 = 0{\cdot}16\ m^{-1}$ in the fitted zone, according to the Kuttruff formula. The fitting density of the upper region, which was essentially empty but contained a mobile crane, lighting fixtures, and the roof trusswork, was considered by Hodgson [10] to be 0·03 m^{-1}, with absorption coefficient 0·05. The input parameters used in his predictions are listed in Table 4.

Measurements of sound propagation were made by Hodgson [10] in the machine shop in octave bands from 250 to 4000 Hz. The sound source was located at 5 m from one end wall, at half width and 1·5 m above the floor. The receivers were at the same height and at distances of 1, 2, 5, 10, 15, 20, 25, and 30 m from the source along the room center line. By comparing measured *SP*s with those predicted by ray tracing, Hodgson [10] found that, using a fitting absorption coefficient of 0·1, the best-fit fitted-region density of 0·23 m^{-1} gave excellent agreement with experiment at all frequencies.

TABLE 4

Values of parameters used by Hodgson [10] *for ray-tracing prediction of sound propagation in the machine shop*

Parameter	Octave band (Hz)				
	250	500	1000	2000	4000
m (Np/m)	0·0003	0·0005	0·001	0·003	0·006
α (empty room)	0·12	0·10	0·08	0·06	0·06
α (fitted room)	0·21	0·18	0·15	0·14	0·14
Q (upper zone) (mFS^{-1})	0·03	0·03	0·03	0·03	0·03
Q (lower zone) (mFS^{-1})	0·23	0·23	0·23	0·23	0·23
α_f (upper zone)	0·05	0·05	0·05	0·05	0·05
α_f (lower zone)	0·1	0·1	0·1	0·1	0·1

Let us now apply the corrected fitting formula to the above data. The mean fitting dimension was calculated from the dimensions of all of the fittings to be $D_f = 1{\cdot}15$ m, corresponding to $Q' = 0{\cdot}255\,m^{-1}$. This is similar to the value of $0{\cdot}23\,m^{-1}$ found by the best-fit method [10], supporting the validity of the correction formula, equation (11). The variation of fitting density with frequency $Q(f)$ calculated from equation (17) is given in Table 5.

By comparing prediction with experiment for different values of fitting absorption coefficient, the best-fit values shown in Table 5 were found. Note that these decrease with increasing frequency. This suggests that low-frequency absorption mechanisms (such as panels and resonators) dominate high-frequency ones (such as surface porosity), which is not surprising in the case of industrial equipment. Note also that, at all frequencies, the product of frequency-varying fitting density and fitting absorption coefficient is close to the frequency-invariant fitting density of $0{\cdot}23\,m^{-1}$ found by Hodgson [10]; this lends credibility to the approach of Akil and Oldham [11, 12].

The 500-Hz measured and predicted sound-propagation curves are compared in Figure 7. Also shown is the curve predicted using $Q = 0{\cdot}23\,m^{-1}$ and fitting absorption coefficient 0·1 as used by Hodgson [10]. The results are very similar at the other frequencies. The agreement between the three curves is excellent at all frequencies and distances. The agreement is as good using $Q(f)$ and the best-fit, frequency-varying fitting-absorption coefficients as that obtained by Hodgson [10]

TABLE 5

The parameters used for ray-tracing predictions using $Q(f)$

Parameter	Octave band (Hz)				
	250	500	1000	2000	4000
Average $Q(f)$ (mFS^{-1})	0·100	0·142	0·182	0·213	0·232
Average α_f	0·20	0·15	0·12	0·10	0·10

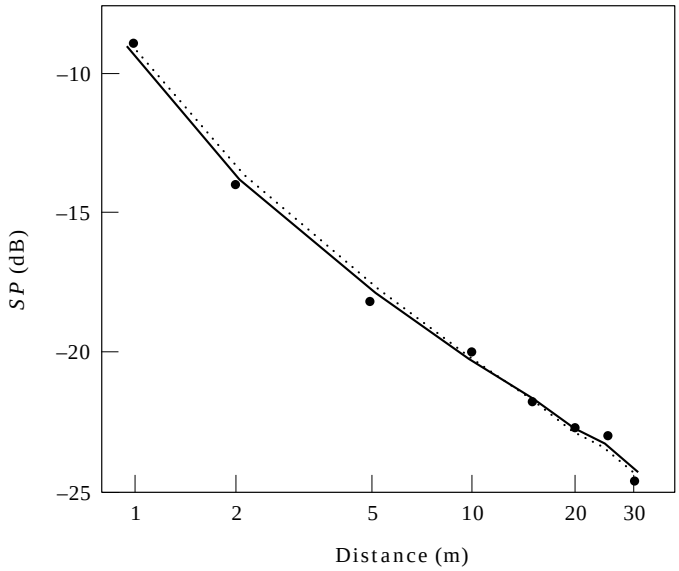

Figure 7. 500-Hz octave-band sound-propagation curves for the fitted machine shop: ●, measured; predicted by ray tracing using fitting densities/absorption coefficients 0·142 m^{-1}/0·15 (· · · · · ·) and 0·23 m^{-1}/0·1 (——).

using constant fitting-absorption coefficient 0·1 and constant fitting density 0·23 m^{-1}. Since the fitting absorption coefficient cannot at present be measured directly, it is not possible to say which set of prediction parameters best represents reality, only that they give equally good agreement with experiment.

7. SUMMARY AND CONCLUSION

A correction formula, equation (11), for calculating the fitting density in the case of large fitting dimensions has been derived, and the magnitude of the correction investigated. The variation of fitting density with frequency was found from sound-propagation measurements in the anechoic chamber. A model, equation (17), to describe the variation, $Q(f)$, was derived from these results using statistical methods. The results suggest that the fitting density calculated by the Kuttruff formula is only valid at some intermediate frequency. At low frequency, fitting densities are smaller than those calculated by the Kuttruff formula; at high frequencies, they are much greater.

The fitting-density models were validated by comparing ray-tracing predictions, using the new parameter values, with experiments in a scale-model workroom and in a full-size machine shop. The validation work strongly supports the new fitting-density model. In the machine shop, the sound-propagation curves were in excellent agreement with the measured values at all distances and frequencies. It was shown that the sound-propagation curves predicted using the Kuttruff formula only agree well with measurement for the cases of sparsely-fitted rooms, or densely-fitted rooms at low frequencies, since in these cases the fitting-density values calculated by the two methods are about same. However, for the case of

densely-fitted rooms with large fittings, the fitting densities calculated using the Kuttruff formula are too small to agree with those measured, especially at high frequencies.

In deriving $Q(f)$, the fitting dimension was taken into account by calculating a fundamental frequency related to dimension. However, only one kind of fitting was used in the project. Since it was not feasible to perform experiments with other fitting dimensions in order to verify the relationship between fitting desity and dimension, this model needs further validation—for example, by measurements in the scale-model workroom with fittings of widely different dimensions, but the same fitting density, and by more measurements in real workrooms.

REFERENCES

1. M. Hodgson 1983 *Applied Acoustics* **16**, 369–391. Measurement of the influence of fittings and roof pitch on sound fields in panel-roof factories.
2. S. Jovicic 1979 *Bericht für das Ministerium für Arbeit, Gesundheit und Soziales des Landes Nordrhein/Westfalen*. Schallausbreitung in Arbeitsgebäuden.
3. E. A. Lindqvist 1982 *Acustica* **50**, 313–328. Noise attenuation in large factory spaces.
4. E. A. Lindqvist 1983 *Applied Acoustics* **16**, 183–214. Noise attenuation in factories.
5. A. M. Ondet and J.-L. Barbry 1989 *Journal of the Acoustical Society of America* **85**, 787–796. Modelling of sound propagation in fitted workshops using ray tracing.
6. S. M. Dance and B. M. Shield 1997 *Journal of Sound and Vibration* **201**, 473–489. The complete image-source method for the prediction of sound distribution in non-diffuse enclosed spaces.
7. M. R. Hodgson 1998 Accepted for publication in *Acustica*. Effective fitting densities and absorption coefficients of industrial workrooms.
8. H. Kuttruff 1967 *Acustica* **18**, 131–143. Über Nachhall in Medien mit unregelmässig verteilten Streuzentren, insbesondere in Hallräumen mit aufgehängten Streuelementen.
9. U. J. Kurze 1985 *Journal of Sound and Vibration* **89**, 365–377. Scattering of sound in industrial spaces.
10. M. R. Hodgson 1989 *Noise Control Engineering Journal* **33**, 97–104. Case history: factory noise prediction using ray tracing—experimental validation and the effectiveness of noise control measures.
11. H. A. Akil and D. J. Oldham 1995 *Journal of Building Acoustics* **2**, 461–481. Determination of the scattering parameters of fittings in industrial buildings for use in computer based factory noise prediction models: part 1—theoretical background.
12. H. A. Akil and D. J. Oldham 1995 *Journal of Building Acoustics* **2**, 527–548. Determination of the scattering parameters of fittings in industrial buildings for use in computer based factory noise prediction models: part 2—scale-model experiments.
13. M. R. Hodgson and R. J. Orlowski 1987 *Journal of Sound and Vibration* **113**, 29–46. Acoustical scale modelling of factories, part I: principles, instrumentation and techniques.
14. M. R. Hodgson 1986 *Proceedings of Inter-Noise* '86, 1319–1323. Towards a proven method for predicting factory sound propagation.